

Differential Detection of Tumor Cells using A Combination of Cell Rolling, Multivalent Binding, and Multiple Antibodies

Ja Hye Myung¹, Khyati A. Gajjar¹, Jihua Chen², Robert E. Molokie^{1,3,4}, and Seungpyo Hong^{1}*

Departments of Biopharmaceutical Sciences¹ and Medicine³, University of Illinois, Chicago, IL 60612

Center for Nanophase Materials Sciences², Oak Ridge National Laboratory, Oak Ridge, TN 38831

Jesse Brown VA Medical Center⁴, Chicago, IL 60612

*All correspondence should be addressed to:

Prof. Seungpyo Hong, Ph.D.

Department of Biopharmaceutical Sciences

College of Pharmacy

The University of Illinois at Chicago

833 S. Wood St. Rm 335

Chicago, IL 60612

List of Sections in Supporting Information

1. *Characterization of the functionalized surfaces using X-ray photoelectron spectroscopy (XPS)*
2. *Characterization of the functionalized surfaces using conventional and energy filtered transmission electron microscopy (TEM)*
3. *Cellular responses of each cell line on the antibody- and E-selectin-immobilized surfaces under flow*
4. *Optimization of surface micropatterning*
5. *Cellular responses of each cell line on the interfaces between antibody- and E-selectin-stripes under flow*
6. *Cell enrichment using the micropatterned surfaces without E-selectin-mediated cell rolling*
7. *Blood sample preparation using Ficoll-Paque Plus*

1. Characterization of the functionalized surfaces using X-ray photoelectron spectroscopy (XPS)

The surfaces were characterized as described in our previous publications.^{1,2} An Axis 165 X-ray photoelectron spectrometer (Kratos Analytical, Manchester, U.K.) equipped with a monochromatic AlK α source ($h\nu = 1486.6$ eV, 150W) and a hemispherical analyzer was used. The % mass concentrations were obtained from high-resolution spectra of the C 1s, O 1s, N 1s, and S 2p regions at an X-ray irradiating angle of 30° at 80 eV of energy and a step size of 0.5 eV, carried on 5 scans per each spectrum.

Surface functionalization by protein immobilization was confirmed using XPS, as summarized in Table S1. The immobilization of aEpCAM, aHER-2 and aPSA was quantitatively confirmed by an increase in carbon and nitrogen compositions as well as a decrease in silicon from the underlying glass substrate, as shown in Table S1. The data also indicate that all surfaces immobilized with proteins had a high degree of surface coverage, as evidenced by the lack of visible underlying silicon. The measured nitrogen content likely corresponds to the degree of protein coverage on the glass surface as the nitrogen composition increased when the total amount of proteins immobilized was increased.

Table S1 Measured atomic compositions of functionalized slides by XPS.

(mass conc. %)	Control	aPSA	aHER-2	aEpCAM
C 1s	28.1	34.6	41.8	42.2
N 1s	0.5	5.4	5.8	5.3
O 1s	55.2	47.0	40.0	39.7
Si 2p	16.2	13.0	12.4	12.8
(C+N)/(O+Si) ratio	0.4	0.7	0.9	0.9

2. Characterization of the functionalized surfaces using conventional and energy filtered transmission electron microscopy (TEM)

TEM samples are prepared on 20-nm-thick silicon wafer based TEM windows (Dune Sciences). Three different types of wafers were functionalized by conjugation with each antibody: i) carboxylate-functionalized silicon wafers; ii) PEGylated wafers; and iii) G7 PAMAM dendrimer-immobilized wafers. The silicon wafer functionalization was followed by the surface functionalization on the epoxy slide.³ Briefly, the carboxylate-functionalized silicon wafers were activated using an 1:1 mixture of 1-ethyl-3-(3-dimethylaminopropyl) carbodiimide (EDC) and *N*-hydroxysuccinimide (NHS) for 1 hr, followed by direct surface conjugation of the antibodies. For the PEGylated surface, the carboxylated silicon wafers activated by EDC/NHS were incubated with PEG (NH₂-(PEG)₅₀₀₀-COOH, Nektar Therapeutics (Huntsville, AL)) at a concentration of 0.5 µg/mL in DDI water for 4 hr, followed by conjugation with antibody solutions after EDC/NHS activation. The dendrimer-coated silicon wafers were prepared on the PEGylated grids. After activation of carboxylic termini of PEG using an 1:1 mixture of EDC/NHS, partially carboxylated G7 PAMAM dendrimers (50 µM in PBS buffer (pH 9.0)) were immobilized on the silicon wafers. The dendrimers immobilized on the silicon wafer were then activated using EDC/NHS, followed by conjugation with antibodies. For all antibody conjugation reactions, a concentration of 5 µg/mL (except for aPSA, which was at 10 µg/mL) was used and was allowed for reaction overnight. All surface functionalization reactions were carried out at room temperature. The volumes of all reagent solutions were fixed at 5 µL, and the surfaces between each step were washed with DDI water or PBS buffer three times to remove the extra reagents from the silicon wafers.

Conventional and energy filtered TEM experiments were conducted using a Zeiss Libra 120 with an in-column Omega-shaped energy filter. TEM experiments were performed at 120kV with an emission current of ~5µA from a LaB6 filament. During the imaging process, a minimal electron dose condition was used and the samples were carefully monitored to eliminate any electron-beam-induced sample damage. Carbon maps were generated with the conventional three-window method, with two pre-edge windows chosen for background prediction and the post-edge window for signal extraction.

Conventional and energy filtered TEM were performed on samples with COOH-functionalized, silicon wafer based substrates, which have a number of 20-nm-thick electron-transparent viewing windows. Conventional TEM (Fig. S1) is based on contrast from electron density. The darker regions represent

the areas with higher electron densities, which include contributions from thickness variation and elemental composition. To better identify the nanoscale distribution of the three different antibodies on PEG and G7 functionalized silicon wafers, we also used energy filtered TEM to generate carbon maps (Fig. S2). In the carbon maps, the brighter spots represent higher carbon content. G7 functionalized surfaces obviously have more intense carbon signals than their PEG functionalized counterparts, suggesting more antibody immobilization.

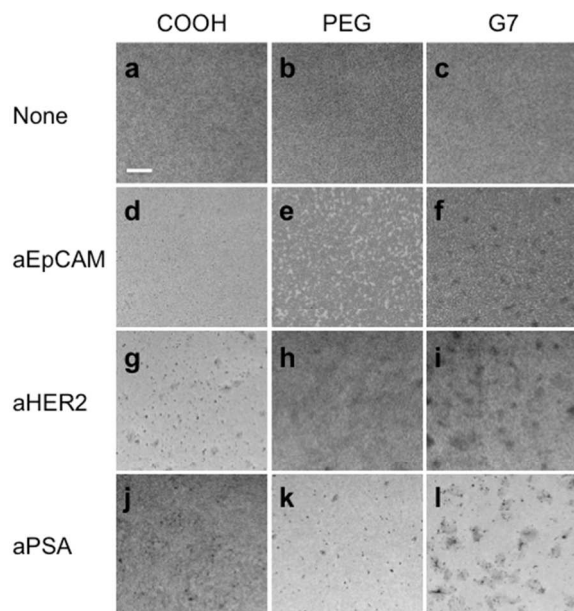


Figure S1 Unfiltered (conventional) bright-field TEM images. Scale = 200 nm

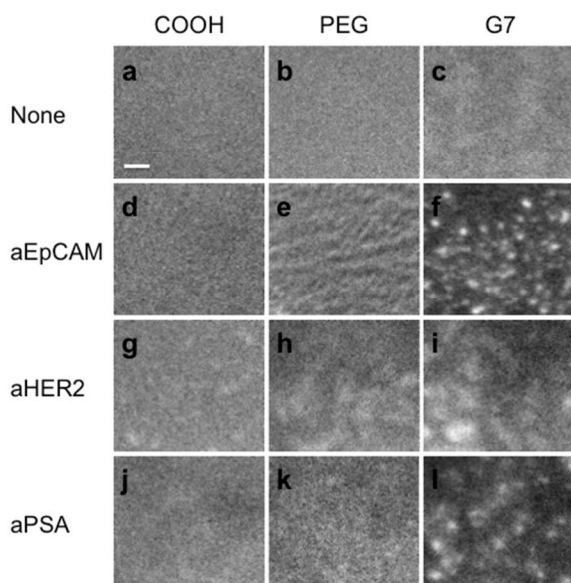


Figure S2 Carbon maps generated from energy filtered TEM. Scale = 200 nm

3. Cellular responses of each cell line on the antibody- and E-selectin-immobilized surfaces under flow

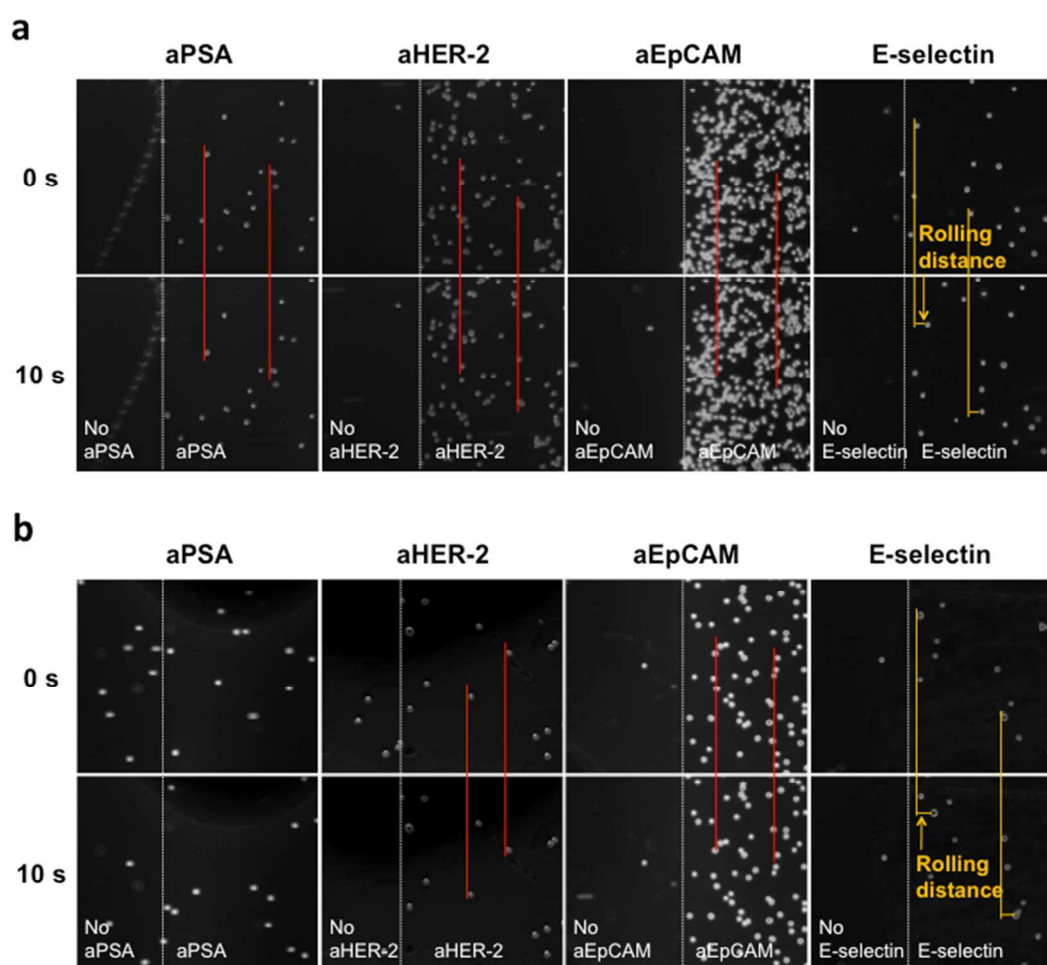
MDA-MB-361 cells were cultured in Leibovitz's L-15 media (Gibco, Invitrogen, Grand Island, NY) supplemented with 1% (v/v) Penicillin/Streptavidin (P/S) and 20% (v/v) FBS, under humidified atmosphere containing 100% air and 0% CO₂ at 37°C. MCF-7 cells were cultured in DMEM media (Cellgro, Mediatech, Manassas, VA) supplemented with 10% (v/v) FBS and 1% (v/v) penicillin/streptomycin (P/S). MDA-PCa-2b cells and HL-60 cells were cultured in BRFF-HPC1 media (AthenaES, Baltimore, MD) and IMDM media (Gibco), respectively, and the both media were supplemented with 20% FBS and 1% (v/v) P/S. All cell lines were purchased from ATCC (Manassas, VA). All of the cancer cell lines except MDA-MB-361 cells cultured in a 37°C humidified incubator containing 95% air and 5% CO₂.

A typical flow chamber experiment was performed as described in our earlier report¹. Briefly, a glass slide functionalized by protein immobilization, a gasket (30 mm (L) × 10mm (W) × 0.25 mm (D), Glycotech, Gaithersburg, MD), and a rectangular parallel plate flow chamber (Glycotech) were assembled in line under vacuum. To observe cellular interactions with the biofunctionalized surfaces, individual cell lines (MDA-PCa-2b, MDA-MB-361, MCF-7, and HL-60) at a concentration between 10⁶-10⁷ cells/mL in the complete media were injected into the flow chamber at a shear stress of 0.2 dyn/cm² using a syringe pump (New Era pump Systems Inc., Farmingdale, NY). Note that, in this flow chamber, 50 μL/min of flow rate is correspondent to 0.2 dyn/cm² of a wall shear stress, 20 s⁻¹ of a wall shear rate, and 50 μm/sec of near-wall non-adherent cell velocity according to the Goldman equation.⁴. Cellular responses of each cell line on each antibody-immobilized surface were monitored using a parallel flow chamber using an Olympus IX70 microscope (IX 70-S1F2, Olympus America, Inc., Center Valley, PA) equipped with a CCD camera (QImaging Retiga 1300B, Olympus America, Inc.).

Cellular responses of all cancer cell models and HL-60 on each antibody-immobilized surface were monitored under flow. Each set of Fig. S3 shows the cellular responses of each cancer cell line on aPSA, aHER-2, and aEpCAM-coated surfaces at t = 0 s (a randomly-picked starting time for recording during the flow experiment) and 10 s (10 sec after the starting time). MDA-PCa-2b cells were stationary bound on all of the three antibody-immobilized surfaces under flow (Fig. S3a). Although MDA-MB-361 cells showed no binding to the aPSA-immobilized surface, the cells were stationary bound on the other two surfaces, aHER-2 and aEpCAM-immobilized surfaces (Fig. S3b). MCF-7 cells were stationary bound only on the aEpCAM-immobilized surface, not on the other surfaces functionalized with aPSA and

aHER-2 (Fig. S3c). Unlike other cancer cell lines, HL-60 cells exhibited no interaction with any antibody-immobilized slides, traveling the flow path in the chamber at the speed of free stream velocity (Fig. S3d).

On the E-selectin-immobilized surface, all cell lines including HL-60 cells exhibited stable rolling, although the rolling velocities of each cell line varied (Fig. S3). The average rolling velocities of MDA-PCa-2b, MDA-MB-361, and MCF-7 cells were 3.1 ± 0.2 , 6.4 ± 0.4 , and 3.2 ± 0.2 $\mu\text{m}/\text{sec}$, respectively. Generally, the rolling velocities of cancer cell lines were faster than those of HL-60 (0.1 ± 0.1 $\mu\text{m}/\text{sec}$) on the E-selectin-immobilized surfaces.



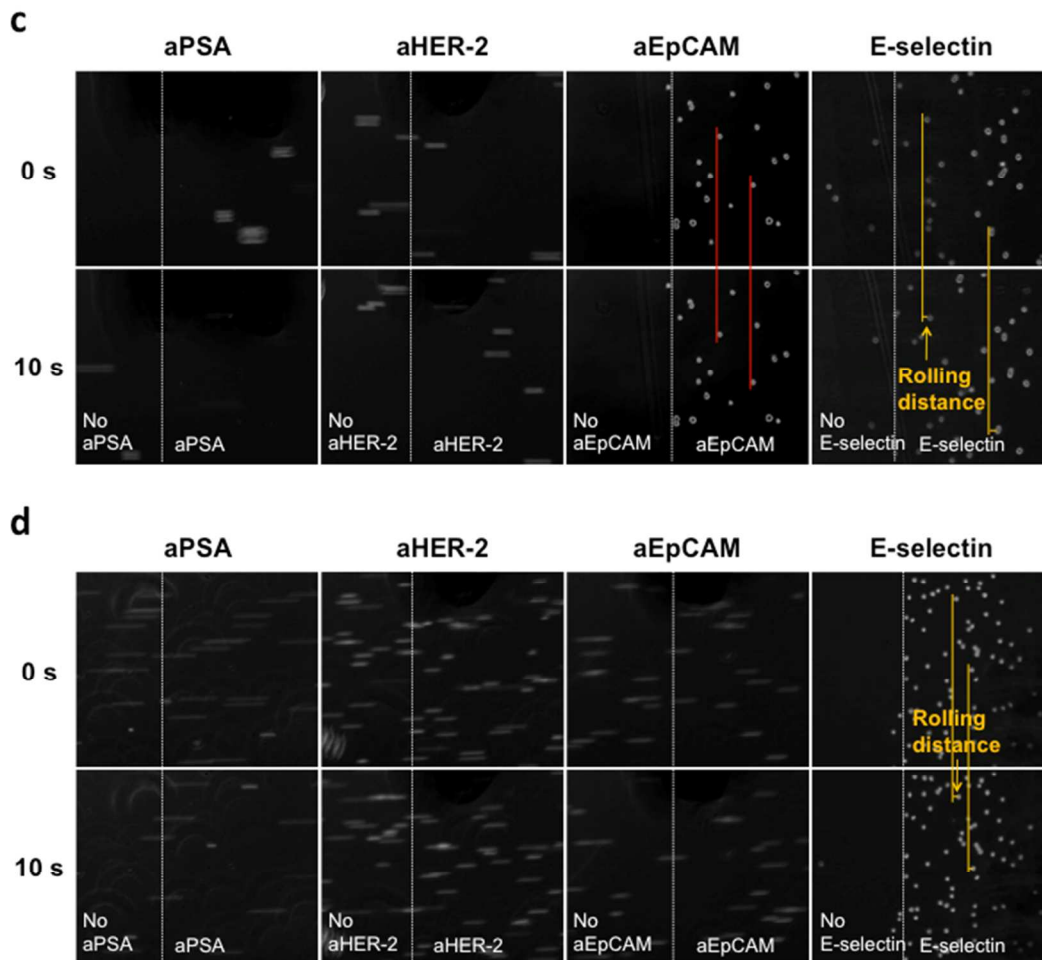


Figure S3 Time-course images of four different cell lines under a shear stress of 0.2 dyn/cm^2 on the surfaces functionalized with various proteins. (a) MDA-PCa-2b, (b) MDA-MB-361, and (c) MCF-7 all showed the stationary binding on the antibody-immobilized surfaces in a cell surface marker-dependent manner. (d) HL-60 cells, in contrast, do not exhibit surface interactions with the antibody-immobilized surfaces. All cell lines, including HL-60 cells, were observed to roll under flow on E-selectin-immobilized surface. The rolling velocities of MDA-PCa-2b, MDA-MB-361, MCF-7, and HL-60 cells were 3.1 ± 0.2 , 6.4 ± 0.4 , 3.2 ± 0.2 , and $0.1 \pm 0.1 \text{ } \mu\text{m/sec}$, respectively. Flow directions of the three sets are from left to right.

4. Optimization of surface micropatterning

The feasibility of the PDMS gaskets to define the area for antibody immobilization was confirmed using FITC-conjugated BSA. A PDMS gasket was used to define the area of an epoxy functionalized glass slide, and the epoxy-functionalized glass surfaces functionalized with FITC-BSA were monitored using a fluorescence microscope at 10× magnification. As the channel width in the PDMS gasket was increased, the width of the FITC-BSA stripes with green fluorescence was proportionally increased (Fig. S4). For surface micropatterning, PDMS gaskets with four channel widths ranging from 100 μm to 1,000 μm were selected.

Effect of the surface patterning with E-selectin and aEpCAM was examined by a quantitative analysis using MDA-MB-361 cells. Fluorescence-labeled MDA-MB-361 cells were injected into a flow chamber for one cycle, consisting of forward flow (pushing) for 5 min and backward flow (withdrawing) for 5 min at 50 $\mu\text{L}/\text{min}$ (0.2 dyn/cm^2). The surface was then washed using PBS buffer for 10 min and using EGTA/ Mg^{2+} -included PBS buffer for 3 min, both at 200 $\mu\text{L}/\text{min}$ (0.9 dyn/cm^2). The number of captured cells on the antibody-immobilized stripe defined using FITC-BSA was counted. The number of captured cells on the aEpCAM patterns with various dimensions was counted and presented in fold enhancement compared to the number obtained using 100 μm -wide aEpCAM pattern (for Fig. S5a) and 500 μm -wide aEpCAM pattern (for Fig. S5b) without E-selectin treatment. Capturing of MDA-MB-361 cells on the aEpCAM-immobilized stripes were increased as an increase of the aEpCAM-pattern width, irrespective of E-selectin treatment (Fig. S5a). However, we used 500 μm -wide patterns for aEpCAM immobilization due to huge variations of capturing efficiencies on 1 mm-wide patterns. When the aEpCAM-immobilized stripes were at 500 μm in width, the capture efficiency on the aEpCAM-stripes was decreased if the E-selectin-stripes were wider than 2 mm (Fig. S5b). Both Fig. S5a and b using the aEpCAM/E-selectin-micropatterned surfaces demonstrated a statistically significant enhancement (up to 147 fold) in MDA-MB-361 capture, as compared to the results using the surfaces with aEpCAM only. Based on these results, the widths of the aEpCAM and E-selectin stripes on the micropatterned surfaces were fixed at 500 μm and 2 mm, respectively.

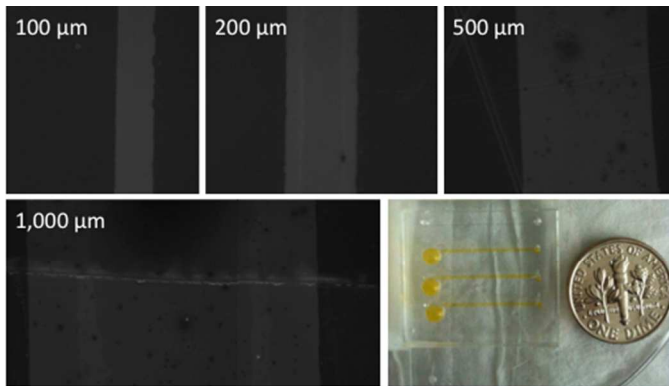


Figure S4 Characterization of the surface micropatterning using FITC-BSA solution. The representative images were taken under a fluorescence microscope at 10 \times magnification. Due to the technical difficulty, two images were merged to show the image for the 1,000 μm -wide pattern.

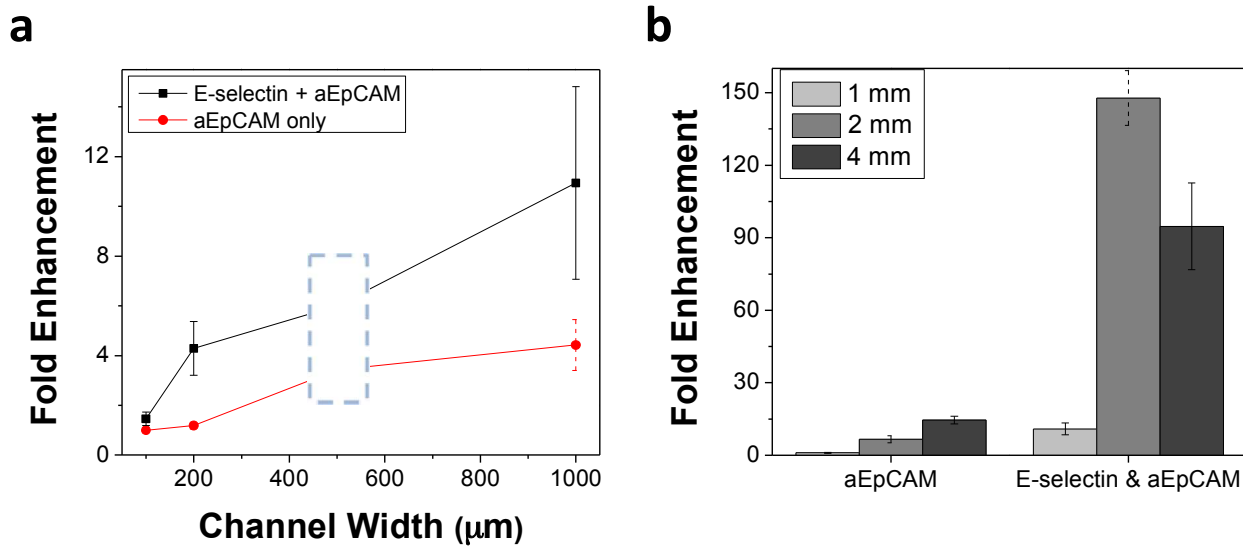
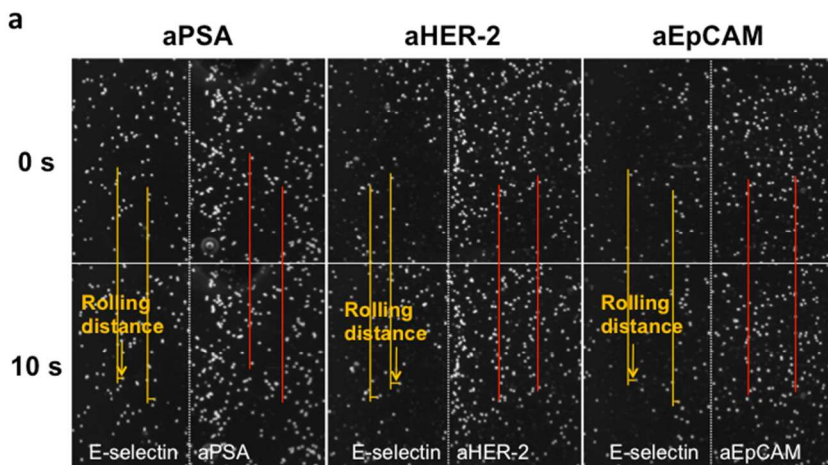


Figure S5 Optimization of the surface micropatterning. (a) The capture efficiency of MDA-MB-361 cell was increased with an increase of the aEpCAM-coated region width, when tested using a surface with pre-coated E-selectin at a width of 2 mm. (b) With the width of the aEpCAM-stripe at 500 μm , the maximum MDA-MB-361 cell capture was obtained on the 2 mm-wide E-selectin-immobilized stripes. Error bars: standard error (n=6).

5. Cellular responses of each cell line on the interfaces between antibody- and E-selectin-stripes under flow

The micropatterned surfaces with three dendrimer-antibody conjugates and E-selectin (defined as a multifunctional surface in this paper) were prepared as described in Methods section. All cancer cell suspensions in the complete cell culture media at 10^6 cells/mL were injected into the flow chamber. We monitored cellular responses of the cancer cells on the interfaces between E-selectin and antibody during PBS washing at a shear stress of 0.9 dyn/cm^2 . All cells on the surface were monitored using an Olympus IX70 inverted microscope with fluorescence light, and images were recorded by a CCD camera using a $4\times$ objective.

The sequential responses of rolling and capturing on the interface between E-selectin and dendrimer-antibody-immobilized stripes were observed under flow. As shown in Fig. S6, all of the cell lines were rolling on the region that functionalized only with E-selectin (the left-hand side of the images), following the flow direction (from left to right). Note that the FITC-BSA-labeled antibody-stripes did not appear in these images taken under natural light. When the rolling cells under flow reached the adjacent dendrimer-antibody-immobilized regions (the right-hand side of the images), the cells were stationary bound in cell surface marker-dependent ways, as shown in Fig. S6. If the target cancer cells have binding affinities to the immobilized antibody, we observed that the cancer cells were accumulated on the boundary of E-selectin and antibody (e.g. MCF-7 cell accumulation on the boundary of E-selectin and aEpCAM in Fig. S6c). The induced cell rolling by E-selectin enhanced the surface detection sensitivity toward MCF-7 cells as they started binding to aHER-2 (Fig. S6c).



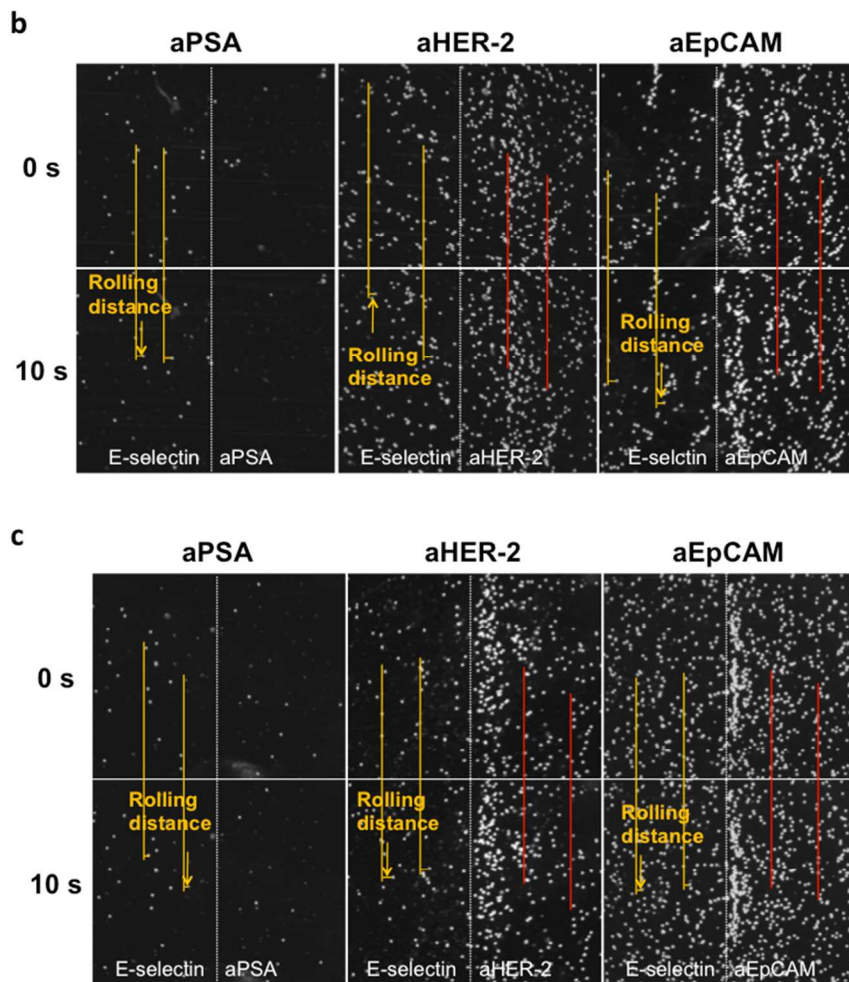


Figure S6 Time-course images of a) MDA-PCa-2b, b) MDA-MB-361, c) MCF-7 cells on the surface interfaces functionalized with antibodies and E-selectin under shear stress of 0.9 dyn/cm^2 . All cells exhibited the rolling behavior on the E-selectin-coated surface, whereas showed stationary binding on the antibody-coated surface in a cell surface marker-dependent manner. The flow direction was from left through right.

6. Cell enrichment using the micropatterned surfaces without E-selectin-mediated cell rolling

We then investigated if the micropatterned surfaces can be used to enrich the cancer cells in a cell surface marker-dependent way. To evaluate separation of the multiple cell populations in the mixtures (1:1:1 (v/v/v)), each cell line was labeled with a fluorescent dye as follows; MDA-PCa-2b with Calcein AM (green), MDA-MB-361 with Cell Alive Blue dye (blue), and MCF-7 with Cell Alive Blue dye (red). The composition percentage in the bound cell population on each antibody-stripe without E-selectin treatment was quantitatively measured (Fig. S7). The composition percentage on the antibody-stripes, especially MDA-PCa-2b cells on the aPSA stripes, clearly shows the surface marker-dependent cell enrichment. However, the detection of the micropatterned surface without E-selectin was not sensitive enough to capture the cancer cells with relatively low expression of the markers (i.e. no binding of MCF-7 cells on the aHER-2-stripe).

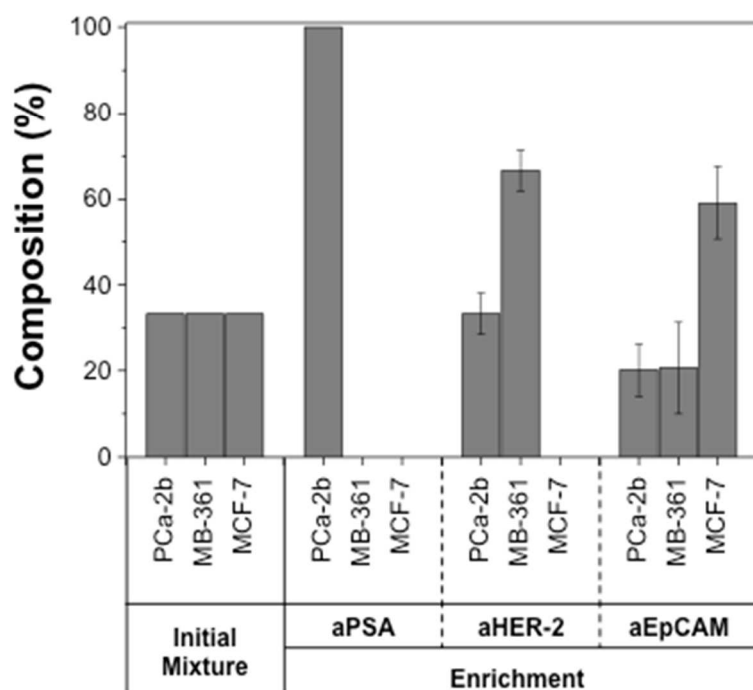


Figure S7 Cell separation and enrichment from cell mixture in a cell surface marker-dependent manner. Compositions (%) of each cell line in the initial cell mixture and the bound cells on each antibody stripe without E-selectin were quantitatively measured. The surface marker-dependent cell enrichment was achieved on the antibody-coated surfaces, especially MDA-PCa-2b cells on the aPSA

stripes. Images and composition percentages were obtained after injection of mixture of the three cell populations (1:1:1 (v/v/v)) onto the surfaces of antibodies only, without E-selectin.

7. Blood sample preparation using Ficoll-Paque Plus

All multifunctional surfaces with multiple antibodies were prepared by sequential addition of dendrimers, antibodies, and E-selectin as described in Methods Section. For the experiments using the blood samples, potential non-specific binding was blocked by surface treatment with 1 $\mu\text{g}/\text{mL}$ methoxy PEG-NH₂ (Nektar Therapeutics) solution, instead of using BSA.

Cancer cell-spiked blood samples were prepared as follows. Cells at a concentration of 1×10^6 cells/mL (5 mL) were seeded onto 25cm² T flask one day before the experiment. Live MDA-PCa-2b, MDA-MB-361, and MCF-7 cells were labeled with fluorescence dyes as described in the previous Section 6. The labeled cells were detached from the surface using TrypLE™ Express (Gibco BRL, Grand Island, NY, USA) to make suspensions at a concentration of 1×10^5 cells/mL in the whole blood withdrawn from healthy donors. The tumor cell-spiked blood samples were prepared at a ratio of 1 tumor cell in the background of 10^4 white blood cells and 10^7 red blood cells. The withdrawn blood was kept at 4°C in a refrigerator and the experiments were performed within 48 hr after the blood-drawing. On a round bottom-tube, a sequence of the following solutions was loaded without mixing following the instruction from the vendor: 3 mL of Ficoll-Paque Plus (Stemcell Technologies Inc., Vancouver, Canada) and 3 mL of the cancer cell-spiked whole blood diluted in 3 mL of PBS buffer (9 mL in total volume). The PBS buffer was supplemented with 2% FBS and 95 USP unit heparin. The round bottom-tubes were centrifuged at 20°C for 20 min at $1,500 \times g$ with brake function off. The upper plasma layers were removed without disturbing the plasma-Ficoll interphase. Three milliliters of mononuclear cell layer at the plasma-Ficoll interphase (buffy coat) were transferred into a new round bottom-tube without disturbing erythrocyte/granulocyte pellets in the bottom layer. The buffy coat including cancer cells was washed twice with the FBS/heparin-included PBS buffer for 10 min at 2,000 rpm with brake function on. The recovered cells were suspended with 3 mL of the complete cell culture media. The cell suspensions were injected into the flow chamber as described in the previous Section 3.

The multifunctional surfaces successfully captured the target cancer cells from the blood samples. The cancer cells spiked into blood were recovered using Ficoll-Paque Plus, and the recovery yields of the three cancer cell lines from blood ranged between 10-20% (Fig. S8). Based on the recovery yield of the cancer cells from blood samples using Ficoll-Paque Plus, the capture efficiency of the multifunctional surfaces were calculated. The fold enhancement of capture efficiency on the multifunctional surface was significantly higher than that of the micropatterned surface only with antibodies under the same

conditions (Fig. S9). The E-selectin treatment was significantly augmented the surface capture efficiency. Importantly, the synergetic effect of cell rolling and multivalent binding was most effective in cancer cell capture.

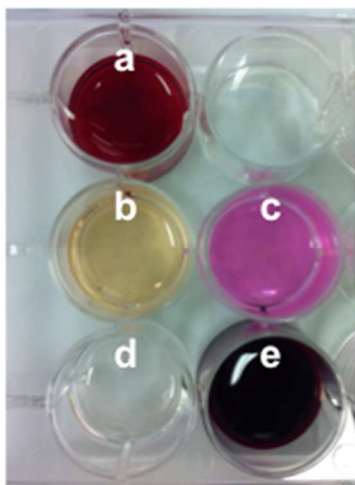


Figure S8 Blood separation using Ficoll-Paque Plus. (a) Cancer cell-spiked whole blood withdrawn from healthy donors, (b) separated plasma (b), buffy coat with MCF-7 cells (c), Ficoll solution (d), and erythrocytes (e). Note that the mononuclear cells including cancer cells and leukocytes were collected into the buffy coat layer.

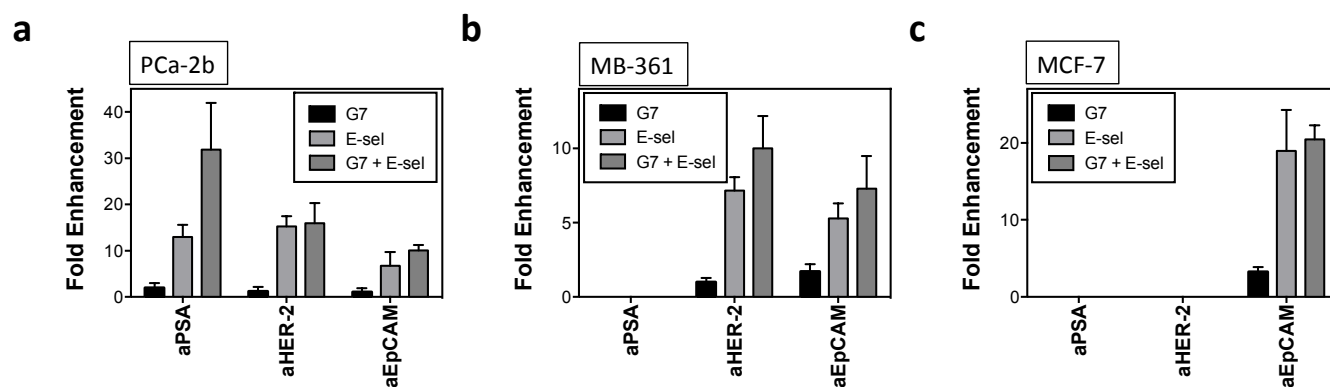


Figure S9 Comparison of cell capture efficiency among the surfaces using cancer cell-spiked blood specimens. Fold enhancements of three different cell lines, such as (a) MDA-PCa-2b, (b) MDA-MB-361, and (c) MCF-7 cells, were compared. Detection sensitivity of the multifunctional surfaces with dendrimers and E-selectin was significantly improved, by up to 32 fold, compared to that of the surfaces

with antibody stripes only. The surface marker-dependent bindings of cancer cell models were also observed. *Fold enhancements for some conditions could be not measured due to no binding of the cells on certain antibodies without E-selectin. Error bars: standard error (n=4).

Movie S1 Sequential cellular responses of cell rolling and stationary binding on the interfaces between antibody- and E-selectin-stripes.

Movie S2 Efficient removal of rolling cells on the E-selectin-stripe using EGTA-included PBS buffer washing.

Movie S3 Cellular responses of the cancer cells recovered from blood samples on the multifunctional surface.

Movie S4 Rolling of natural leukocytes recovered from blood samples on the multifunctional surface.

REFERENCES

- (1) Myung, J. H.; Launier, C. A.; Eddington, D. T.; Hong, S. *Langmuir* **2010**, *26*, 8589-8596.
- (2) Hong, S.; Lee, D.; Zhang, H.; Zhang, J. Q.; Resvick, J. N.; Khademhosseini, A.; King, M. R.; Langer, R.; Karp, J. M. *Langmuir* **2007**, *23*, 12261-12268.
- (3) Myung, J. H.; Gajjar, K. A.; Saric, J.; Eddington, D. T.; Hong, S. *Angew. Chem. Int. Ed. Engl.* **2011**, *50*, 11769-11772.
- (4) Goldman, A. J.; Cox, R. G.; Brenner, H. *Chemical Engineering Science* **1967**, *22*, 653-660.